Evaluation of NCEP-GFS-based Rainfall Forecasts over the Nagavali and Vamsadhara Basins in India

G Venkata Rao,[a] Venkata Reddy Keesara,[a] Venkataramana Sridhar,[b] Raghavan Srinivasan,[c] N. V. Umamahesh,[a] Deva Pratap,[b]

[a] *Department of Civil Engineering, National Institute of Technology Warangal, Telangana, 506004, India*

[b] *Department of Biological Systems Engineering, Virginia Polytechnic Institute and State University, Blacksburg, VA*

[b] *Director of Spatial Sciences Laboratory, Agrilife Research, Texas A&M University, College Station, TX*

Corresponding author: Venkataramana Sridhar, vsri@vt.edu

ABSTRACT

Rainfall forecasting and its spatio-temporal variability is important for many hydrological applications. It is critical to understand the uncertainty and verify the quality of rainfall forecasts provided by Numerical Weather Prediction (NWP) models. In the present study, the National Center for Environmental Prediction (NCEP) Global Forecast System (GFS) model performance was evaluated for day-1 to day-5 forecast with a threshold of 1 mm/day over both the Nagavali and Vamsadhara river basins, India. From the results, the model predicted the rainfall with a correlation coefficient of greater than 0.3 and probability of detection greater than 0.6 for day-1 and day-3 forecasts. The bias in rainfall prediction shifted from overestimation to underestimation by 30% as forecast lead time increased. The total mean error was decomposed into hit, false, and missed bias. The main sources of total mean error are hit bias and false bias. However, missed bias influenced total mean error as lead time increased. Bias correction was applied for the rainfall events with a rainfall intensity greater than 12 mm/day. RMSE improved by more than 18% for day-1 forecast in both the Nagavali and Vamsadhara basins, and the improvement ranged between 3% to 9% for other days. In the Nagavali basin, BIAS and ME improved and ranged from 44% to 65% for day-1 to day-5 forecast, whereas in the Vamsadhara basin, it ranged from 65% to 93%. Our findings are useful for early warning dissemination during the flood events, resource mobilization to protect communities, and sustainable water resources planning and management.

Keywords: Rainfall; Extreme events; GFS; Bias Correction

1. Introduction

Rainfall is the most important natural weather element for climate analysis, water resources management, monitoring of extreme weather events, and flood forecasting (Prakash et al. 2018; Rao et al. 2020b; Bisht et al., 2017a; Bisht et al., 2017b; Ning et al. 2017; Damrath et al. 2000; Sun et al. 2018; Deng et al. 2018). Rainfall forecasts are currently provided using conventional methods such as satellite observations, weather radars, and numerical weather prediction (NWP) models. Among these observations, satellites and weather radars provide qualitative forecasts, while NWP models provide quantitative forecasts (Sridevi et al., 2020). Hence, quantitative rainfall forecasts from NWP models that represents land-atmospheric interactions continue to be the primary source of rainfall data for input into any hydrological model for flood forecasting, water management and disaster assessments among other applications (Sridhar, 2013; Shahrban et al. 2016; Sujatha and Sridhar, 2018; Sridhar and Valayamkunnath, 2018). NWP forecasts were first used in Europe and the United States, but are now used all over the world (Saulo et al., 2001). The National Centre for Medium-Range Weather Forecasting (NCMRWF) is the nodal agency for weather forecasting in India. At the present, the NCMRWF provides weather forecasts with a resolution of 0.25°× 0.25°, which are used by the India Meteorological Department (IMD) for operational forecasting (Mukhopadhyay et al., 2019; Sridevi et al., 2018).

The forecasts provided NWP model do not measure directly rainfall intensity. Instead, rainfall is estimated based on the measured quantities. Because of the high spatio-temporal variability of rainfall, the NWP model forecasts provided have comparatively lower forecasting skill in forecasting surface parameters (Sridevi et al., 2018). As a result, rainfall forecasts must be validated before they can be used as inputs to any rainfall-runoff model for soil moisture, streamflow, evapotranspiration and drought applications (Sridhar et al. 2006; Sridhar et al. 2013; Shahrban et al. 2016; Sridhar et al. 2019). The degree of similarity between the forecast and observed condition is used to determine the quality of the forecast (Durai and Bhowmik, 2014; Saulo et al., 2001). Forecasts from the NWP model can be validated using either the measure- or distribution-oriented forecasts verification methods. Both approaches represent different aspects of forecast quality, and their benefits can be used to gain better understanding the NWP model's forecasts and highlight unique strengths (Singh et al., 2014). If the

verification approaches are properly designed, the NWP model verification results can meet the needs of hydro-meteorological and operational forecasting agencies.

Several studies had examined the skill of rainfall forecast by various NWP models, including the Limited area Analysis and Forecast System (LAFS) (Bhowmik et al., 2007), the Global Spectral Model (GSM) running at NCMRWF (Mandal et al., 2007), the National Center for Environmental Prediction (NCEP) Global Forecasting System (GFS) (Dube et al., 2014; Durai et al., 2010; Durai and Bhowmik, 2014; Ganai et al., 2021; Mukhopadhyay et al., 2019; Prakash et al., 2016b; Sharma et al., 2015; Sridevi et al., 2020, 2018), the Regional Meso-Scale Weather Simulation Model (MM5 Model) (Singh et al., 2014), and the UK Met Office Unified Model (Ashrit et al., 2020; Dube et al., 2014; Durai et al., 2015; Satyanarayana and Kar, 2016; Sharma et al., 2017) over the Indian region. Using various accuracy and skill measures, Durai et al. (2010) evaluated the skill of GFS five-day rainfall forecasts and concluded that the model is capable of predicting the presence of rainfall rather the magnitude and location. Durai and Bhowmik (2014) verified the prediction skill of the GFS T574 and GFS T1534 models over the Indian region during the 2011 summer monsoon season. They reported that both models are skilful in predicting rainfall, specific humidity, and lower tropospheric wind circulation. However, the magnitude of error for these parameters increased as the forecast lead time increased. Sharma et al. (2015) evaluated the medium range rainfall forecasts of NCMRWF's Global Forecast System (NGFS) over the Indian region and found that the rainfall pattern error contributes more to rainfall forecast error than location and volume errors. Durai et al. (2015) verified quantitative forecasts from four operational Ensemble Prediction System (EPS) (ECMRWF, UKMO, NCEP - GFS, and JMA) over India. They found that EPS could reproduce seasonal mean rainfall over climatologically heavy rainfall regions. The forecast skill of NCEP and UKMO appeared to be similar to the ensemble mean forecast of EPS. Prakash et al. (2016) evaluated the skill of the GFS T574 and GFS T1534 models over South Asia during peak monsoon months. They reported that GFS T1534 performed marginally better than GFS T574. Similar findings were reported by Sridevi et al. (2020, 2018) for the Indian region.

Based on previous studies, it is clear that the skill of rainfall forecasts from NWP models has been verified over India, and that the models are capable of capturing rainfall over various climatological regions. Though the models are able to capture rainfall, the accuracy in predicting location and magnitude varies considerably which causes systematic bias in forecasting rainfall (Yang et al., 2020). This may be attributed to model physical parameterization flaws, uncertainties in initial and boundary conditions, grid resolution,

complex atmosphere-ocean-land-ice interactions (Cho et al., 2020; Prakash et al., 2016b). Hence, post-processing of rainfall forecasts to reduce the bias may be required for operational purposes. The most commonly used post-processing methods are neural network method (NN), logistic regression (LR), Bayesian model average (BMA), model output statistic method (MOS), Kalman filter (KF), running mean, and others (Durai and Bhradwaj, 2014; Fan and Van, 2011; Yang et al., 2020; Zarei et al., 2021). Although every bias correction method has its pros and cons, there is no perfect method. For instant, MOS requires long training periods from a static model, while NN and BMA require large computational resources. In addition to that, now a days NWP model centers make frequent changes to numerical procedures, physical parameterizations and model resolutions (Durai and Bhradwaj, 2014). To overcome this ever changing NWP model base, Ebert (2001) introduced the concept of frequency matching method (FMM). The method has the capability to apply dynamic bias correction and requires less computational resources. Since 2004, FMM has been implemented to bias correct GFS provided rainfall forecasts at NCEP in the United States (Zhu. and Toth, 2004). Many studies have demonstrated that, FMM is good enough to bias correct the rainfall forecasts over the region of interest (Guo et al., 2021; Wang et al., 2020; Yang et al., 2020; Zhu and Luo, 2015). Wang et al., (2020) suggested that applying bias correction to the rainfall forecasts at basin level may improve the forecast accuracy. Hence, for any hydro-meteorological applications, the NWP model forecasts at the basin level need to be verified rather than on country level for making better decisions.

This study is focused mainly to evaluate the forecasting skill of GFS T574 model provided forecasts over the Nagavali and Vamsadhara basins which are located in the eastern India. Both the basins play an important role in meeting the irrigation and water supply demands in south Odisha and north Andhra Pradesh states of India. Over the years, an increasing trend was observed in rainfall and rainfall extremes in both basins. In the Nagavali basin rainfall has increased at rate of 4 mm/decade in the monsoon season, whereas in the Vamsadhara basin rainfall has increased at a rate of 9 mm/decade. A very slight increase was observed in the magnitude of rainfall extremes at decadal scales (Rao et al., 2020b). Setti et al. (2020) reported an increase of 100 mm in annual average rainfall over the past 20 years. There are frequent floods in the delta areas of both Nagavali and Vamsadhara basins as a result of heavy rainfall in during the monsoon season, cyclonic activities in the pre- and post-monsoon seasons, and the presence of hilly terrains in the uplands of both the basins. Over the past two decades, the frequency and intensity of prolonged floods has increased and caused severe damage to crops,

life, and property in the delta regions of both basins (DC, 2017). According to state government records, there were more than 12 flood events in Nagavali basin and 9 flood events in Vamsadhara basin due to extreme rainfall events (APSDMA, 2017). Hence, precise and accurate rainfall forecasts will help the farmers in planning their day-to-day agricultural operations, and the government agencies in issuing early warnings during flood events in the delta regions of the Nagavali and Vamsadhara basins. This investigation is being conducted as part of the framework development for real-time flood forecasting using the Soil and Water Assessment Tool (SWAT) over the Nagavali and Vamsadhara basins. The study area, methodology, and results are presented in the following sections.

2. Study Area

The Nagavali and Vamsadhara river basins in India plays an important role in meeting irrigation and water supply demands in south Odisha and north Andhra Pradesh (Fig. 1). The Nagavali and Vamsadhara rivers are two independent, adjacent and interstate eastern flowing rivers that originate in the Kalahandi district of Odisha and run between latitudes of 18° 10′ to 19° 45′ N latitude and longitudes of 82° 54′ to 84° 20′. The total length of the Nagavali river from its headwaters to its mouth in the Bay of Bengal is approximately 256 km, with a catchment area of 9510 square km, and the Vamsadhara river is about 254 km, with a catchment area of 10830 square km. The Nagavali and Vamsadhara basins receive an average rainfall of 1230 mm and 1400 mm, respectively. The people in the catchment area rely primarily on agriculture. Paddy, cotton, red gram, sugarcane, groundnut, and sesame are among the crops grown in the basins during both the Kharif and Rabi seasons.

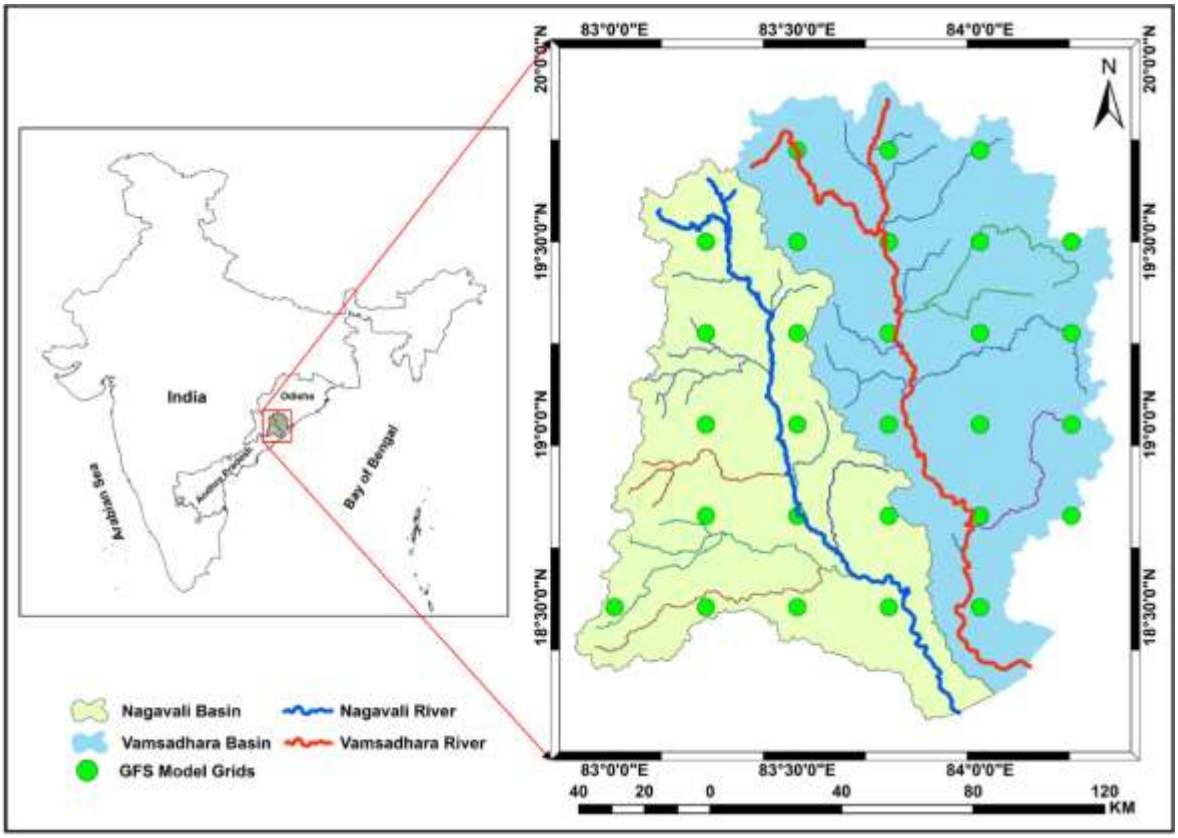

Fig. 1. Geographical Location Map of the Nagavali and Vamsadhara Basins.

3. Data Used

a. Observed Data

For the evaluation of GFS model rainfall forecasts, gridded rainfall data available at a horizontal resolution of 0.25°×0.25° from the India Meteorological Department (IMD) was used. The detailed information about the development of IMD gridded rainfall data is reported in Pai et al. (2014). There are no missing records in the daily rainfall records. IMD gridded data has been verified with the rain gauge data provided by Mahanadi & Eastern Rivers Organization (M&ERO), Central Water Commission (CWC) Bhubaneswar and found a good correlation of 0.79 between them. The detailed information about the verification of gridded rainfall is reported in Rao et al., (2020b).

b. GFS Data

The Global Forecast System (GFS) of the National Center for Environmental Prediction (NCEP) is a medium range hydrostatic NWP model, which provides weather forecasts starting from June 01, 2015. It provides deterministic and probabilistic guidance on weather data for the next 16 days in GRIB2 format. The NOAA Grid point Statistical Interpolation (GSI) 3-D

variational ensemble Kalman filter-variational hybrid system is used by the GFS modelling system for data assimilation (Mccorkle et al., 2018). The GFS files with a horizontal resolution of 0.25°×0.25° were downloaded from the NCAR Research Data Archive. The forecast is updated four times per day (00, 06, 12, and 18 UTC) and includes 3-hour forecasts for the first ten days (i.e., 0 to 240 hours) as well as 12-hour forecasts for the next six days (i.e., 240 to 384 hours). The forecast is updated every 3 or 6-hours and includes rainfall for the next 3 or 6 hours. The rainfall parameter in GFS forecasts is named Total_precipitation_surface_3_hour or 6_hour_accumulation depending on the hour of forecast. In the variable name, 3-hour or 6-hour accumulation indicates the accumulation of rainfall in that 3 hour or 6 hours from the file forecast hour. On June 12th, 2019, the model was updated by adding a new variable called Total precipitation surface mixed intervals accumulation. The new variable provides the accumulated rainfall from the model initialization to the end of the forecast hour in the file. In the present analysis, daily rainfall forecast data from the GFS model were extracted for an area bounded between 18° - 20° N and 82.75° - 84.50° E at 0.25° × 0.25° grid resolution for a period of 2041 days i.e., from June 1, 2015 to December 31, 2020. A total of 28 grids falling over the Nagavali and Vamsadhara basins. Out of which 12 grids are over the Nagavali basin and the remaining over the Vamsadhara basin. The model performance was evaluated using several accuracy and skill measures for 24-hr accumulated rainfall from day-1 to day-5.

4. Methodology

In the present study, verification was carried out for the GFS model against IMD gridded rainfall data at the same resolution (0.25° × 0.25°). Model performance is evaluated using several accuracy and skill measures (Broorks et al., 2017) for day-1 to day-5 forecasts of 24-h accumulated rainfall over the Nagavali and Vamsadhara basins.

a. Statistical Metrics

Statistical metrics such as correlation coefficient (CC), root-mean-square-error (RMSE), mean error (ME), and relative bias (BIAS) are used to quantify the difference between GFS rainfall forecasts and observed data. CC refers to the degree of linear agreement between the forecasted and reference datasets. The absolute average error is measured using RMSE, which gives more weight to larger errors. ME refers to the averaged magnitude differences between the forecasted and reference datasets. Bias measures the average error trend in forecasted rainfall relative to observed rainfall. The mathematical equation for CC, RMSE, ME, and RBIAS are presented below (Prakash et al., 2016a).

201

$$CC = \frac{\sum_{i=1}^{n}(O_i - \bar{O})(S_i - \bar{S})}{\sqrt{\sum_{i=1}^{n}(O_i - \bar{O})^2}\sqrt{\sum_{i=1}^{n}(S - \bar{S})^2}}, \bar{O} = \frac{1}{n}\sum_{i=1}^{n} O_i, \bar{S} = \frac{1}{n}\sum_{i=1}^{n} S_i \quad (1)$$

$$RMSE = \sqrt{\frac{1}{n}\sum_{i=1}^{n}(S_i - O_i)^2} \quad (2)$$

$$BIAS = \frac{\sum_{i=1}^{n}(S_i - O_i)}{\sum_{i=1}^{n} O_i} \times 100 \quad (3)$$

$$ME = \frac{1}{n}\sum_{i=1}^{n}(S_i - O_i) \quad (4)$$

202 Where, *O* is the observed rainfall data, *S* is the GFS forecasted rainfall data, $\bar{O}$ is the mean
203 of observed rainfall, $\bar{S}$ is the mean of the forecasted rainfall, and *n* is the total number of
204 observations.

205 *b. Contingency Statistics*

206 Due to the high spatial and temporal variability of rainfall, the standard method proposed
207 by World Meteorological Organization (MWO) (World Meteorological Organization, 1977) is
208 insufficient for the verification of rainfall forecasts provided by NWP models. For measuring
209 the skill of the NWP model for rainfall forecasts, contingency statistics based on frequency of
210 occurrence are more appropriate (Durai et al., 2010).

211 Contingency statistics are used to evaluate the GFS model's skill to distinguish between
212 the dichotomous estimation. The dichotomous estimation will return 'Yes' if the model predicts
213 rainfall and 'No' if there is no rain. A threshold value is always used to distinguish between
214 rain and no-rain events. Therefore, a threshold of 1 mm/day is considered. The contingency
215 statistics used in the present study are probability of detection (POD), false alarm ration (FAR),
216 critical success index (CSI), and true skill score (TSS). POD measures the fraction of observed
217 rain events that were correctly forecasted by the model. FAR indicates the fraction of forecasted
218 rain events that were observed to be no-rain events. CSI measures the fraction of rainfall events
219 that were correctly diagnosed by the model. TSS measures the ability of the model to
220 distinguish between the occurrence and non-occurrence of an event. The mathematical
221 equations for POD, FAR, CSI, and TSS are presented below (Sharma et al., 2021).

222

$$POD = \frac{H}{H + M} \tag{5}$$

$$FAR = \frac{F}{H + F} \tag{6}$$

$$CSI = \frac{H}{H + M + F} \tag{7}$$

$$TSS = \frac{(H \times CN) - (M \times F)}{(H + M) \times (F + CN)} \tag{8}$$

Where, H is the number of observed rain events that are correctly forecasted, F is the number of rainfall events forecasted but not detected, M is the number of observed rainfall events that are not forecasted, CN is the number of no rainfall events in both the observed and forecasted data. The detailed information about H, F, M and CN are presented in Table 1. The rainfall threshold for calculating these statistics was set at 1mm/day. The day considered as dry if the rainfall was less than 1 mm/day. A wet day is one in which the rainfall exceeds 1 mm/day.

Forecast	Observed	
	Rain	No Rain
Rain	Hit (H)	False (F)
No Rain	Miss (M)	Correct Negative (CN)

Table 1. The contingency classification used to verify the forecasts by calculating Probability of Detection (POD), False Alarm Ratio (FAR), Critical Success Index (CSI), and True Skill Score (TSS) with a threshold of 1 mm/day.

c. Error Decomposition

The error decomposition method was first proposed by Tian et al. (2009). It is used to evaluate the error components in rainfall estimates. The method breaks divides mean error into three independent components: hit bias (HB), missed bias (MB), and false bias (FB). When the mean error is calculated across the entire dataset, it does not provide detailed information about the source of the error. When the mean error is decomposed, the three possible error sources can be distinguished. When rain events are correctly forecasted by the GFS model, but the rainfall intensity is incorrectly estimated, HB occurs. MB denotes the error caused by rain events that were incorrectly forecasted as no-rain events. The error caused by no-rain events that are incorrectly forecasted as rain events is referred to as FB. The value of HB can be either

positive or negative, where MB is always negative and FB is always positive. The mathematical expressions for the HB, MB, and FB are given as follows (Deng et al., 2018):

$$HB = \frac{1}{n}\sum_{h=1}^{H}(S_h - O_h) \quad (9)$$

$$MB = -\frac{1}{n}\sum_{m=1}^{M} O_m \quad (10)$$

$$FB = \frac{1}{n}\sum_{f=1}^{F} S_f \quad (11)$$

$$Total\ Bias\ (TB) or\ Mean\ Error\ (ME) = HB + MB + FB \quad (12)$$

Where, n is the total number of observations, H is the total number of hit events. M is the total number of missed events, and F is the total number of false events.

The sum of HB, MB, and FB is always equal to mean error. As the MB and FB always have opposite signs, they may cancel each other out, resulting in a smaller mean error than individual components. Therefore, breaking down the mean error into independent components may aid us in better understanding the error nature of forecasted rainfall and the uncertainties of retrieval processes.

d. Bias Correction

Accurate rainfall estimates have the potential to reduce uncertainty in hydrological simulations. GFS rainfall forecast bias was corrected out using a simple multiplication bias correction scheme. The bias factor (BF) was calculated as the ratio of gridded rainfall to GFS rainfall forecasts. To obtain bias corrected rainfall estimates, the GFS rainfall forecasts were multiplied by the BF. The mathematical expression for calculating the BF were given below (Lekula et al., 2018):

$$BF = \frac{\sum_{i=1}^{n} O_i}{\sum_{i=1}^{n} S_i} \quad (13)$$

Where, *i* is the grid location and *n* is the total number of grids analyzed.

Following bias correction, the skill score (SS) of BIAS, RMSE, and ME were calculated with respect to the reference value to find if there was any improvement in the model forecast.

Skill score was the relative accuracy score of the a forecast over a reference value (Rao et al., 2020a). The mathematical expressions were given below for calculating the SS for BIAS, RMSE, ME:

$$SS_{BIAS} = 1 - \frac{BIAS_{after\ bias\ correction}}{BIAS_{before\ bias\ correction}} \quad (14)$$

$$SS_{RMSE} = 1 - \frac{RMSE_{after\ bias\ correction}}{RMSE_{before\ bias\ correction}} \quad (15)$$

$$SS_{ME} = 1 - \frac{ME_{after\ bias\ correction}}{ME_{before\ bias\ correction}} \quad (16)$$

5. Results and Discussions

a. Characteristics of Statistical Indices

The box plots of statistical indices (CC, BIAS, RMSE, and ME) of GFS rainfall forecasts from day-1 to day-5 against IMD rainfall over the Nagavali and Vamsadhara basins are presented in Fig. 2 and 3, respectively. From the box plots of CC, it was observed that the day-1 forecasts have shown highest correlation in both basins and gradually decreased with an increase in lead time. The decrease in CC with the increase in lead time may be attributed to the variations in the Sea Surface Temperature (SST) and rainfall relationship. As the lead time increases, the relationship between SST and rainfall shifts from positive to negative because of the periodic forcing imposed by the northward propagating monsoon intra seasonal oscillations (Sahai et al., 2013). Durai and Das, (2019) suggested that the rainfall forecasts from NWP models with a CC greater than 0.3 are considered good. In both basins, the magnitude of CC for day-2 and day-3 forecasts is within the acceptable range. From the magnitude of CC, it was observed that, GFS model was able to capture the rainfall forecasts in both basins with a lead time of 3 days. The BIAS values indicated that, on average the GFS model overestimated the rainfall in both the basins. The average overestimation for day-1 forecast is more than 38% in the Nagavali basin and 40% percent in the Vamsadhara basin. In both basins, the overestimation of rainfall has gradually reduced from day-1 to day-3 and then increased on day-4 and day-5. Similar results were obtained for ME in both basins. The random component of the forecast error is measured using RMSE. It showed an average value of approximately 12 mm/day in the Nagavali basin and 14 mm/day in the Vamsadhara basin and no significant changes were found with the increase in lead time.

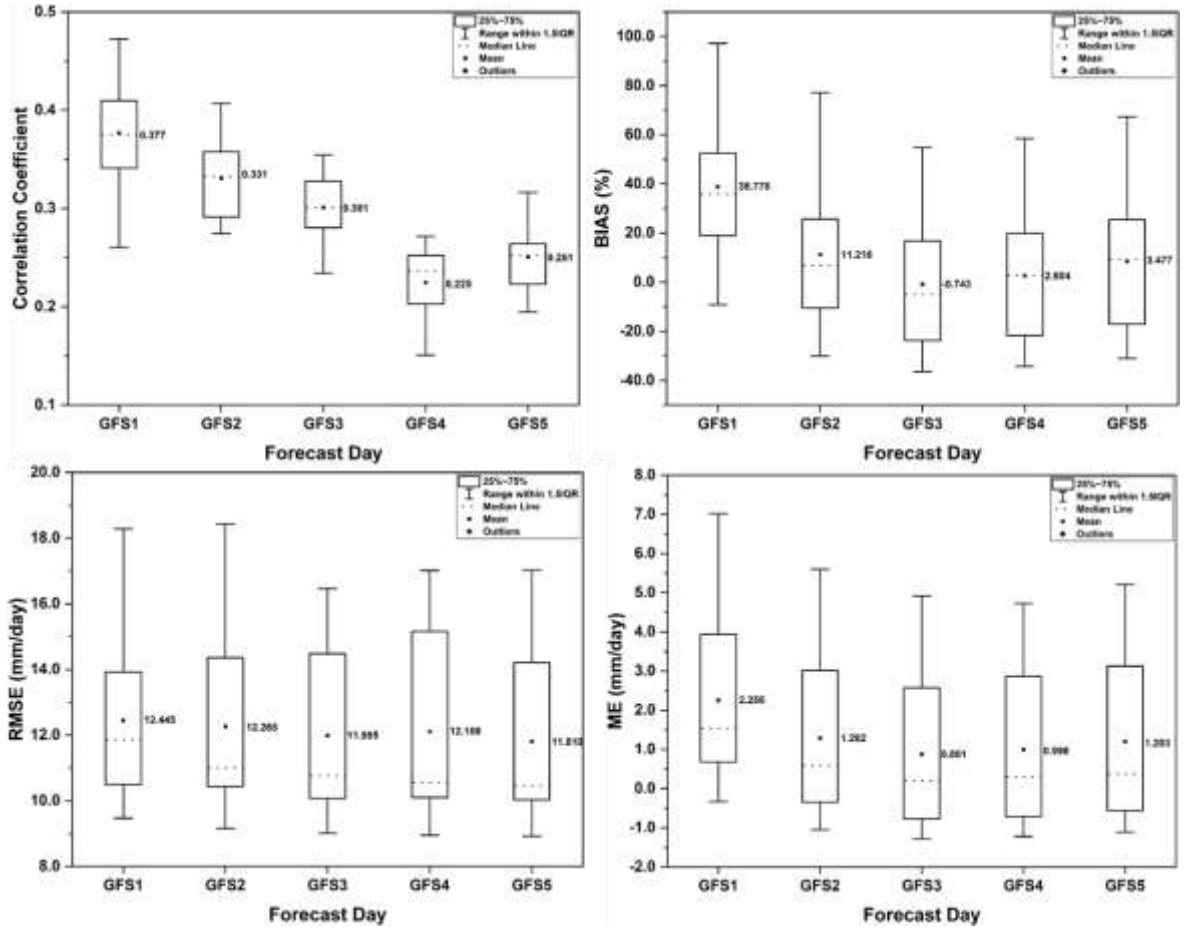

Fig. 2. Box plots of CC, BIAS, RMSE, and ME over the Nagavali basin.

The spatial distribution of statistical indices (CC, BIAS, RMSE, and ME) of GFS rainfall forecasts from day-1 to day-5 is presented in Fig. 2. The magnitude of day-1 CC ranged between 0.3 to 0.5 in both the Nagavali and Vamsadhara basins, with maximum values in the middle and upper portions. Rainfall forecasts from NWP models with a CC greater than 0.3 are considered good (Durai and Das, 2019). The magnitude of CC in both basins decreases as the forecast lead time increases. The magnitude of CC has decreased to less than 0.3 for day-2 to day-5 forecasts in all parts of the Nagavali basin. The magnitude of CC for day-2 and day-3 forecasts is within the acceptable range (greater than 0.3) in all parts of the Vamsadhara basin. In contrast, the magnitude of CC is less than 0.3 in all parts of the basin for day-4 and day-5 forecasts. The CC values show that the trend in rainfall forecasts is in good agreement with observed data in both basins from day-1 to day-3.

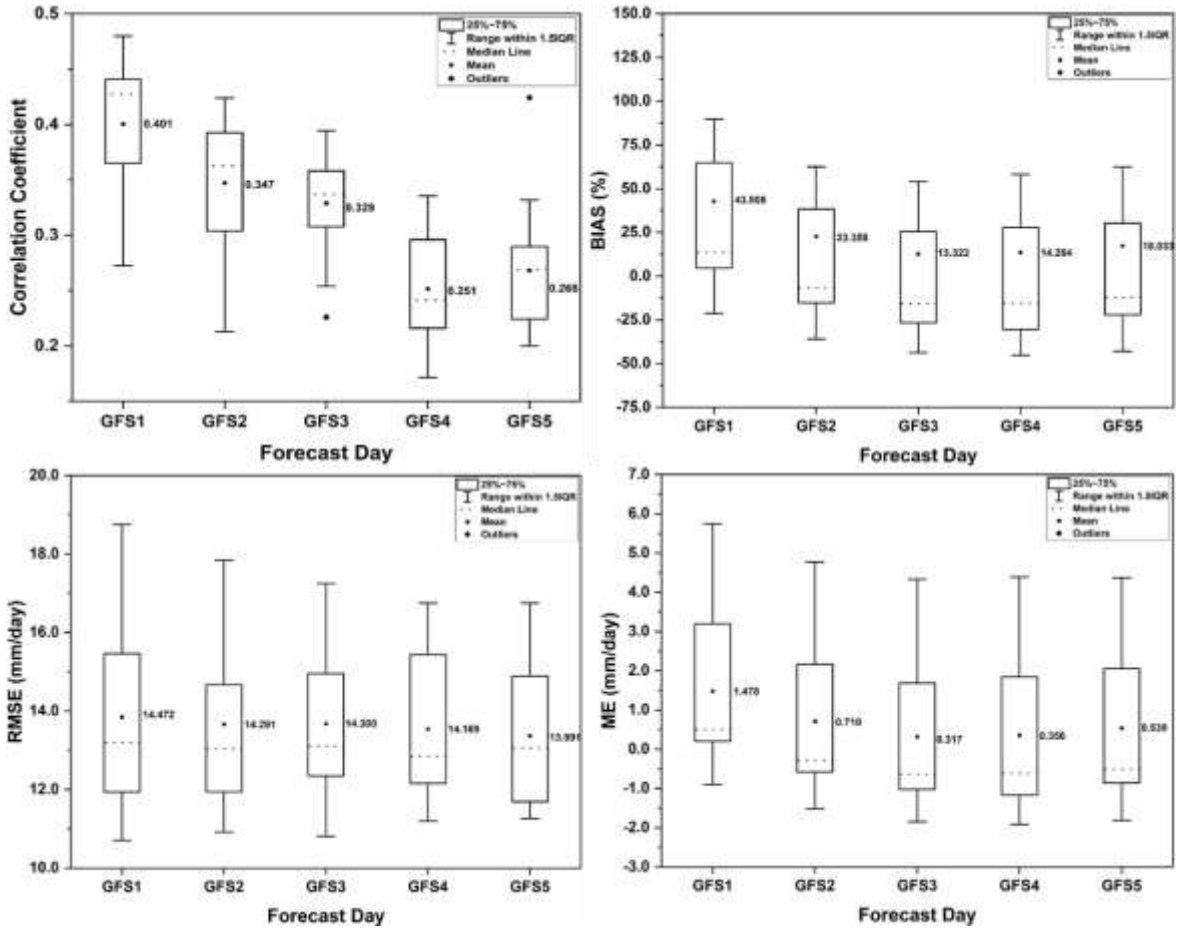

Fig. 3. Box plots of CC, BIAS, RMSE, and ME over the Vamsadhara basin.

From the spatial distribution of BIAS (Fig. 4), the model overestimated the rainfall in the day-1 forecast in most parts of the both Nagavali and Vamsadhara basins. The overestimation for day-1 forecast is between 20%– 80%. Rainfall forecasts shifted from overestimation to underestimation as forecast length increased. The Vamsadhara basin has experienced a shift from overestimation to underestimation. In the Nagavali basin, however, the shift occurred mainly in the lower portion of the basin. The magnitude of RMSE ranged between 9 to 27 mm/day for day-1 to day-5 forecasts. The RMSE displayed similar spatial patterns from day-1 to day-5. In almost all parts of the Vamsadhara basin, RMSE values greater than 12 mm/d have been observed. The spatial distribution of RMSE values from day-1 to day-5 did not differ significantly in the Nagavali basin. However, a decrease in the magnitude of RMSE values was observed throughout the basin. For day-1 to day-5 forecasts, the magnitude of ME ranged between -2 to 12 mm/day. The spatial distribution of ME shows that the highest values (greater than 4 mm/day) of ME were found along the boundary of the Nagavali basin (adjacent to Vamsadhara). Lower ME values (-2 to 4 mm/day) were found in all parts of both basins except along the Nagavali basin's boundary. The magnitude of ME changed from positive to negative

as the forecast lead time increased, but no significant difference was observed in spatial plots of ME from day-1 to day-5. From the results of BIAS and ME, the GFS model overestimated the rainfall forecasts on day-1. The GFS model underestimated the rainfall from day-2 forecast onwards due to the forecast lead time. The findings are consistent with those of Durai and Das (2019).

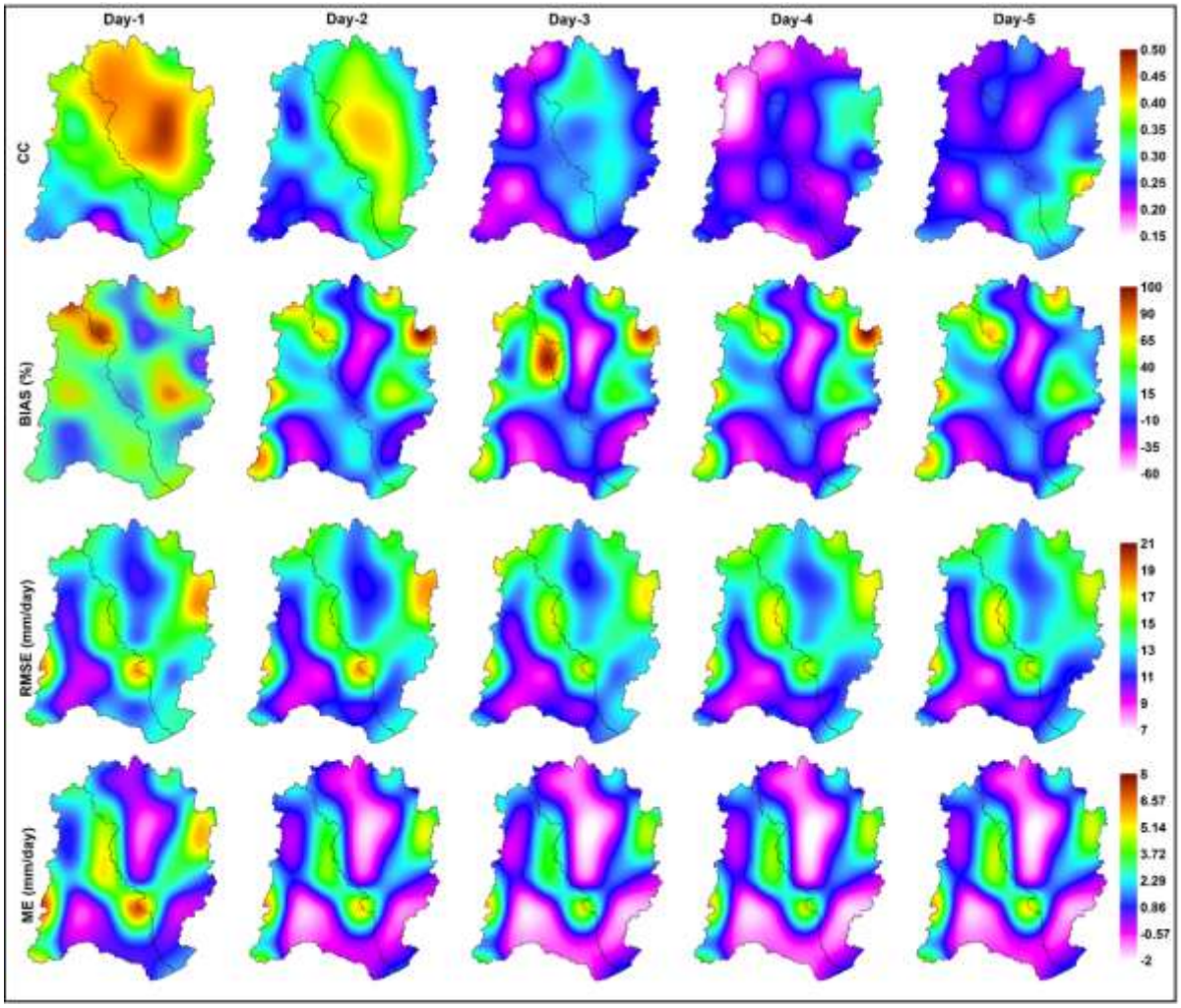

Fig.4. Spatial plot of the Correlation Coefficient (CC), Relative Bias (BIAS), Root Mean Square Error (RMSE), and Mean Error (ME) for the GFS five-day (i.e., day-1 to day-5) rainfall forecast over the Nagavali and Vamsadhara basins.

b. Analysis of Contingency Statistics

The contingency statistics (POD, FAR, CSI, and TSS) of GFS rainfall forecasts from day-1 to day-5 were calculated for yes/no rainfall condition at a threshold of 1 mm/day for both basins (Fig. 5 and 6). From the figures 5 and 6, it was observed that the POD values of GFS forecasts are good and has highest value of 0.783 in the Nagavali basin and 0.759 in the

Vamsadhara basin. A slight decrease in POD values was observed with the increase in lead time. Although there is a decrease in POD values with the increase in lead time, the GFS model was able to capture at least 68% of the rainfall events over the Nagavali basin and 70% of the rainfall events in the Vamsadhara basin. The FAR values indicated that, from day-1 to day-5 forecasts, the GFS model was unable to capture approximately 50% of the rainfall events over the Nagavali basin and 48% of the rainfall events over the Vamsadhara basin. The fraction of rainfall events correctly detected by the model was measured by CSI. The CSI has highest value of 0.423 and 0.435 on day-1 forecast in the Nagavali and Vamsadhara basins, respectively. The values of CSI indicated that the GFS model correctly forecasted nearly 40% of rainfall events. TSS assessed the model's ability to distinguish between the occurrence and non-occurrence of events. From the values of TSS, the ability of GFS model to distinguish between the occurrence and non-occurrence of events is more than 40%.

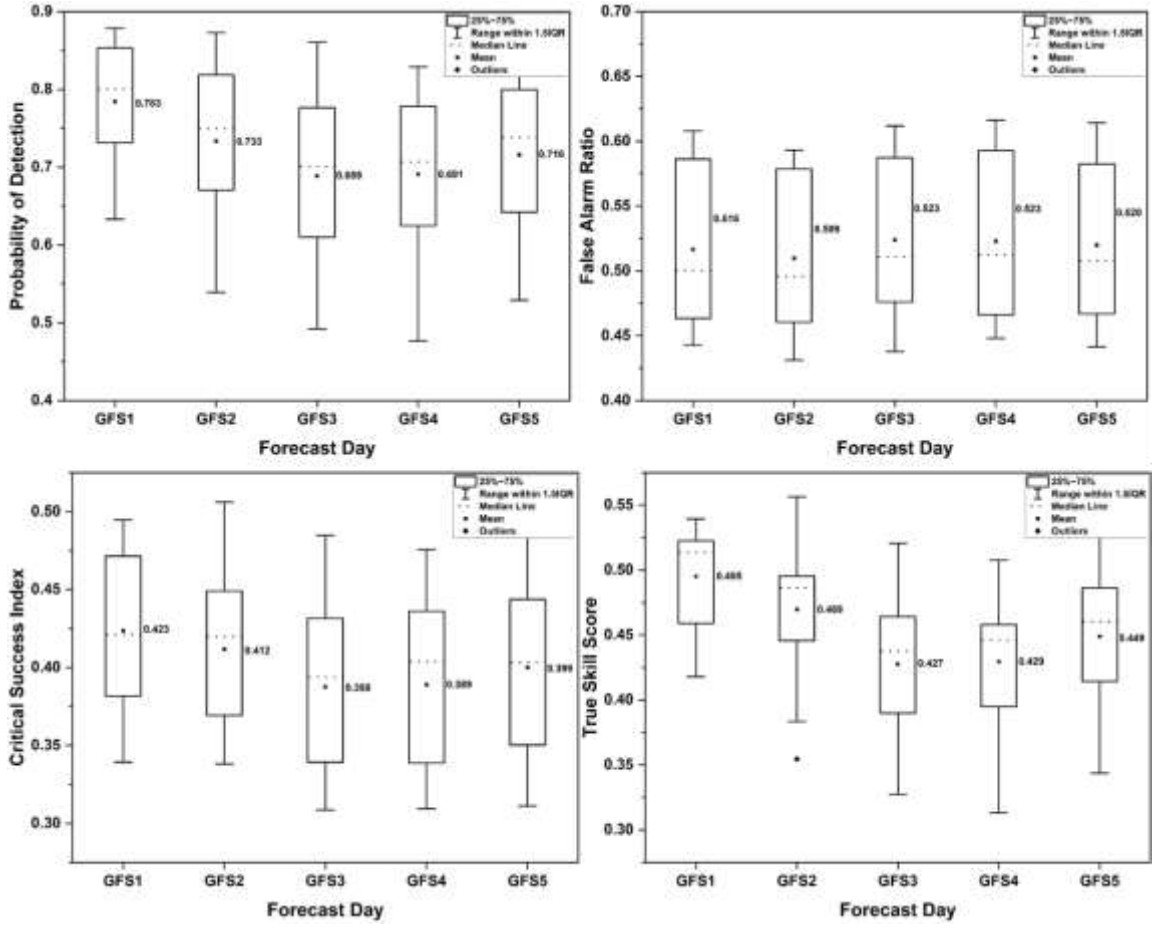

Fig. 5. Box plots of POD, FAR, CSI, and TSS over the Nagavali basin

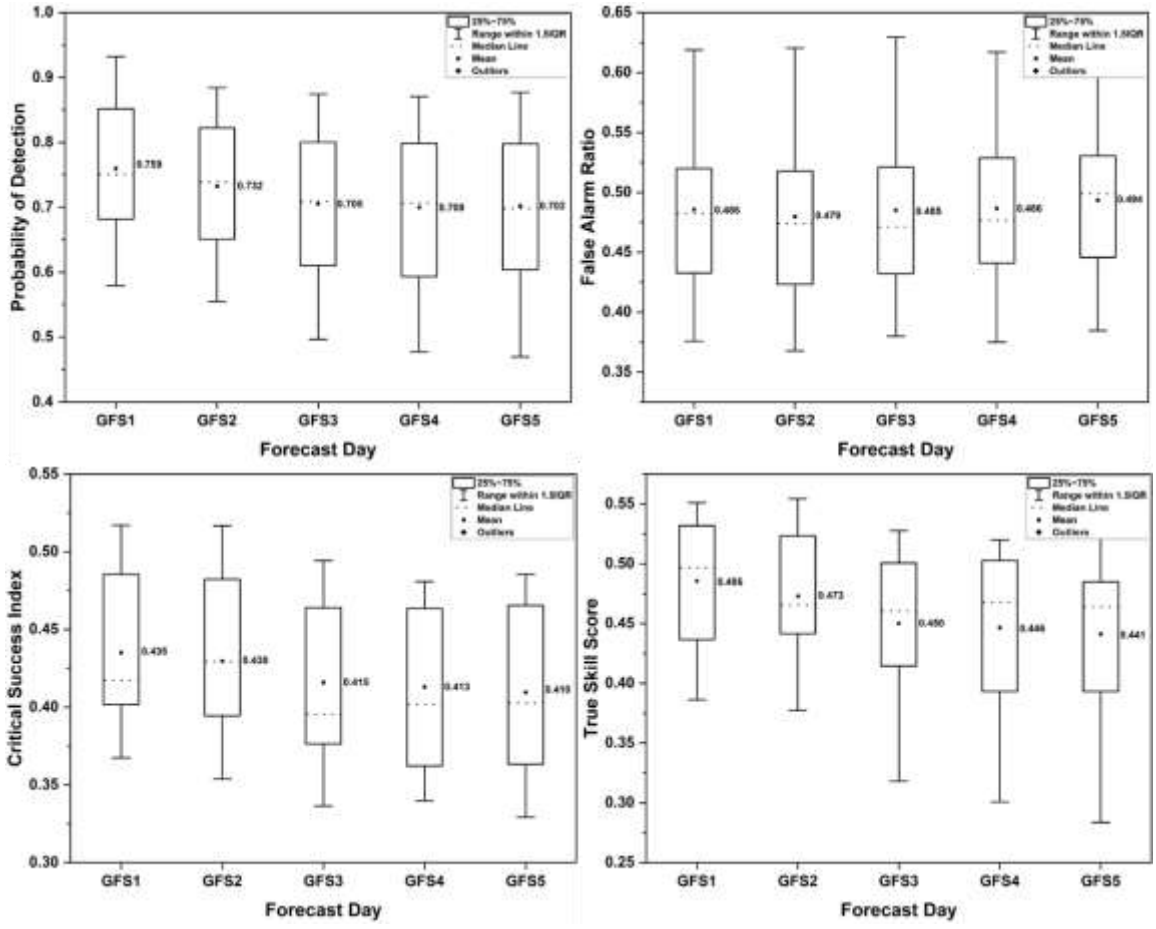

Fig. 6. Box plots of POD, FAR, CSI, and TSS over the Vamsadhara basin

The spatial distribution of contingency statistics (POD, FAR, CSI, and TSS) is presented in Fig. 7. The results show that the POD was greater than 0.6 for a threshold of 1 mm/day in all parts of the Nagavali and Vamsadhara basins for day-1 and day-2 forecast. With the forecast lead time, the POD was decreasing in the lower Nagavali basin and upper middle and upper portion of the Vamsadhara basin. Despite the forecast lead time, the minimum POD values in the Nagavali and Vamsadhara basins were 0.55 and 0.5, respectively. The POD values indicated that the GFS model could detect more than 50% of rainfall events with a five-day lead time.

Higher FAR values of FAR were evident in all parts of the Nagavali basin, except for the upper middle portion. Higher FAR values were found in the lower middle and lower portions of the Vamsadhara basin. Lower FAR values were found in the upper middle and upper portion of the basin. With an increase in forecast lead time, FAR have increased in almost all parts of the basin. The CSI score over most parts of the basin was between 0.4 and 0.5 for day-1 to day-5 forecast. The results shown by CSI were consistent with Durai and Das (2019). The TSS score was more than 0.4 in all parts of both the basins for day-1. The value of TSS decreased

as forecast lead time increased. The lower portion of the Nagavali basin and upper most middle portion of the Vamsadhara basin had the greatest reduction in TSS value. Even with the increased lead time, the GFS model distinguished more than 30% of rainfall events on day-5 forecast.

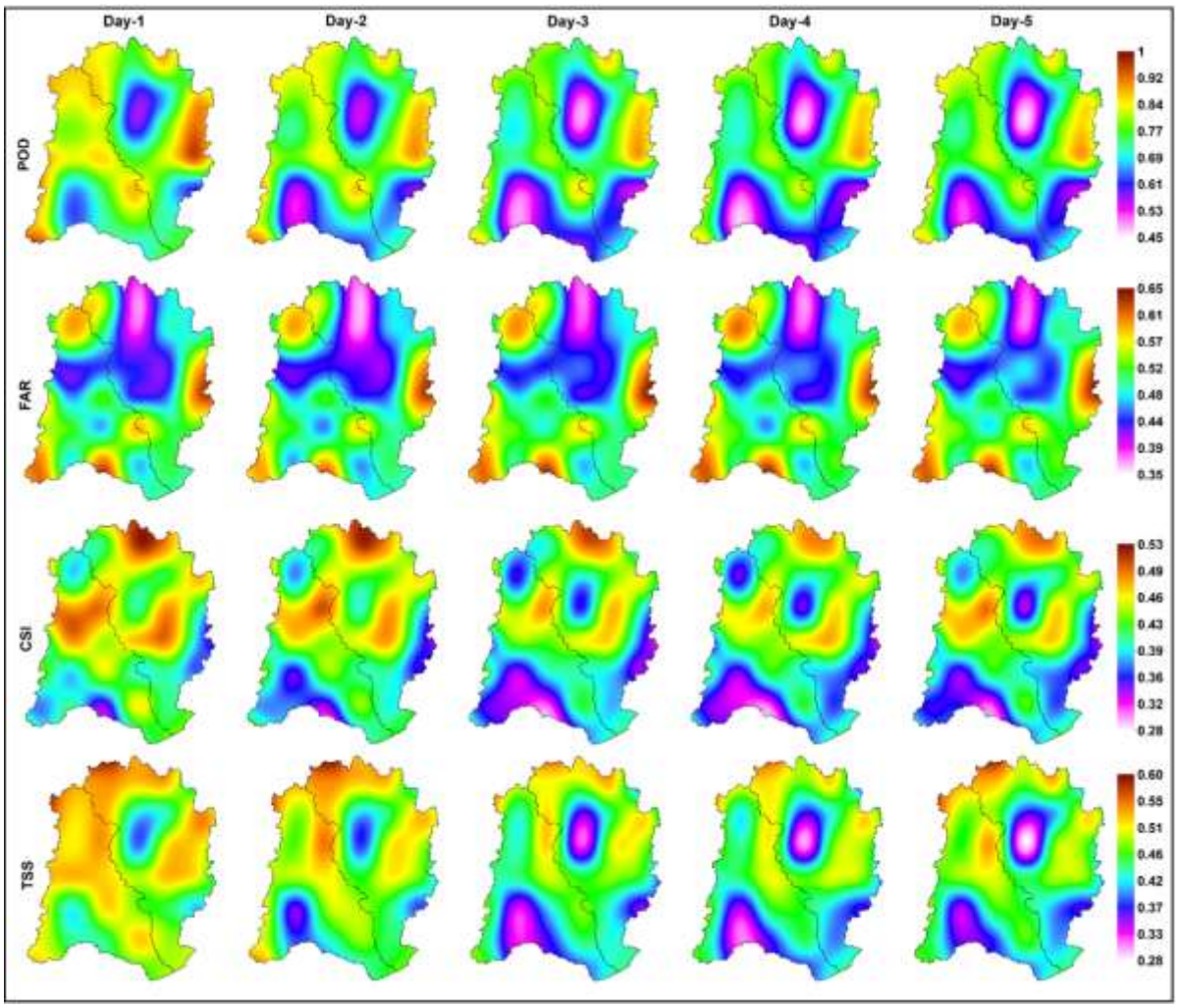

Fig.7. Spatial plot of the Probability of Detection (POD), False Alarm Ratio (FAR), Critical Success Index (CSI), and True Skill Score (TSS) for the GFS five-day (i.e., day-1 to day-5) rainfall forecast over the Nagavali and Vamsadhara basins.

c. Error Decomposition

The total bias of the GFS day-1 to day-5 forecast were decomposed into three independent components: HB, MB, and FB. Box plots are an easy method to express the characteristics of a data set, such as symmetry, outliers, and variance. The box plots for HB, MB, FB and TB are presented in Fig. 8. These biases were calculated for both the Nagavali and Vamsadhara basins using the total daily dataset. From the results, the HB and FB were more dominant than the

MB in GFS rainfall forecasts. The magnitude of HB gradually decreased from day-1 to day-3 forecast and a small increase was observed on day-4 and day-5 forecast. The results obtained by MB and FB are comparable to those obtained by HB.

To further investigate the influence of HB, FB, and MB on total bias, the spatial distribution of the decomposed error components is presented in Fig. 9. From the spatial patterns, it was evident that the spatial distribution of ME was mainly influenced by HB and FB. All of the error decomposed components displayed similar spatial patterns, with a change in magnitude. For day 1 to day 5, the magnitude of HB ranged from -1.6 mm/day to 2.8 mm/day, MB ranged from 0.06 to -2 mm/day, and FB ranged from 0.6 mm/day to 5.3 mm/day. The higher values of HB (greater than 2 mm/day) are located in the lower middle portion of Vamsadhara basin and the middle portion of Nagavali basin along the boundary adjacent to Vamsadhara for day-1 forecast. The magnitude of HB changed from positive to negative as forecast lead time increased, following the same spatial patterns as day-1 forecast. The change in HB from positive to negative suggested that the GFS model forecasts overestimated the rainfall on day-1 and gradually underestimated as lead time increased. Higher MB values were found in the upper middle portion of the Vamsadhara basin along the Nagavali boundary and in the lower portion of the Nagavali basin. With increasing lead time, the magnitude of MB gradually increased. The increase in magnitude of MB indicates that as the forecast lead time increased, so did the number missing events in the GFS model forecasts. The spatial distribution of FB was comparable to that of HB. The magnitude range of FB gradually decreased as forecast lead time increased, from 0.8 mm/day to 5.3 mm/day to 0.6 mm/day to 4.2 mm/day. The decrease in magnitude of FB with forecast lead time indicated a reduction in false events. From the results, HB was always contributing to ME. Compared to MB, FB was the major influencing component of ME at the beginning of the GFS forecast, on the other hand, MB influenced the ME with the forecast lead time.

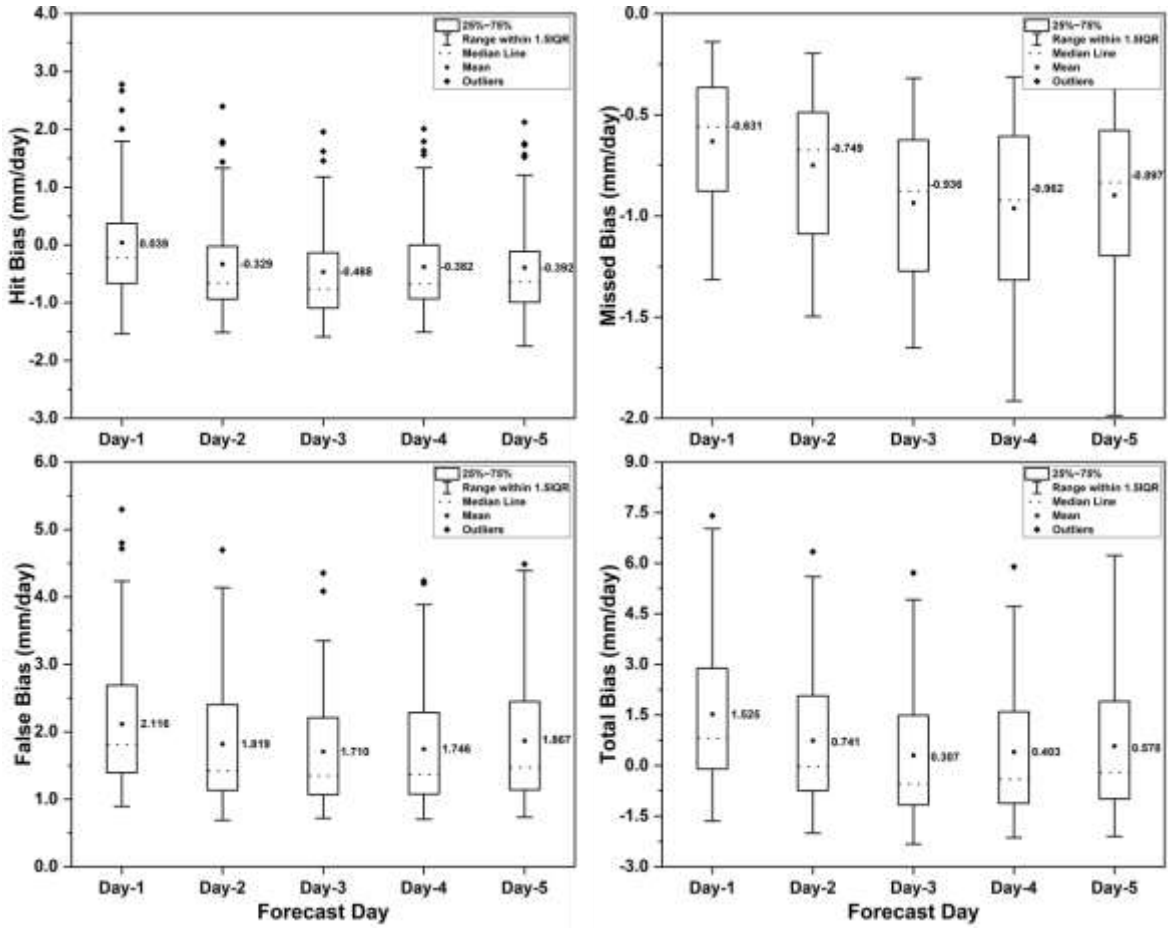

401

402 Fig. 8. Box-plot of the Hit Bias, Missed Bias, False Bias and Total Bias for the GFS five-
403 day (i.e., day-1 to day-5) rainfall forecast over the Nagavali and Vamsadhara basins.

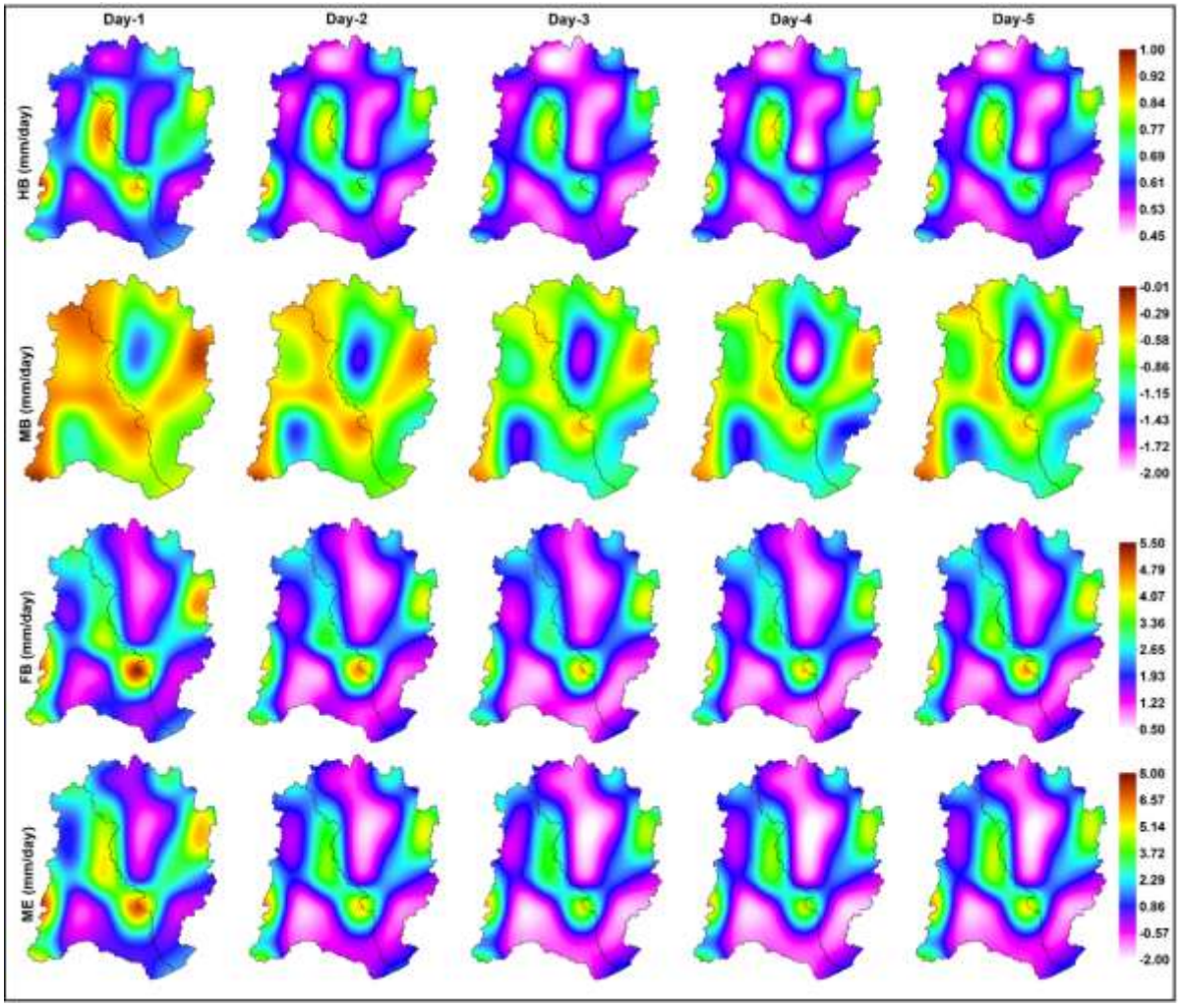

Fig. 9. Spatial plot of the decomposed error components of Hit Bias, Missed Bias, False Bias, and Mean Error for the GFS five-day (i.e., day-1 to day-5) rainfall forecast over the Nagavali and Vamsadhara basins.

d. Intensity Distribution Plots

The intensity distribution of rainfall amount provided unique insights into error dependence on rain rate as well as the potential impact of errors on hydrological applications. This was due to the fact that most hydrological processes, such as surface runoff, were highly sensitive to both the intensity distribution and total rainfall amounts. The intensity distribution was calculated as the ratio of the total amount of rainfall in each bin to the total amount of rainfall observed over the entire study period. Fig. 10 depicts the intensity distribution plots of total, hit, missed, and false rainfall. From the intensity distribution of total rainfall, the GFS model forecasts underestimated the rainfall with rain rate less than 12 mm/day and greater than 64 mm/day. The model, on the other hand, overestimated the rainfall, with rain rates ranging from 12 mm/day to 64 mm/day. The intensity distribution of hit events followed a similar pattern to

the intensity distribution of total rainfall, indicating that hit bias was a significant contributor to total bias. Missed rainfall forecasts ranged from 1 mm/day to 32 mm/day for day-1 to day-5 forecast. The number of missing rainfall events in the forecast gradually increased as the forecast lead time increased. The model forecasted false rainfall was greater than the missed rainfall, with rain rates ranging from 2 mm/day to 64 mm/day. The number of false rainfall events in the forecast gradually decreased as lead time increased.

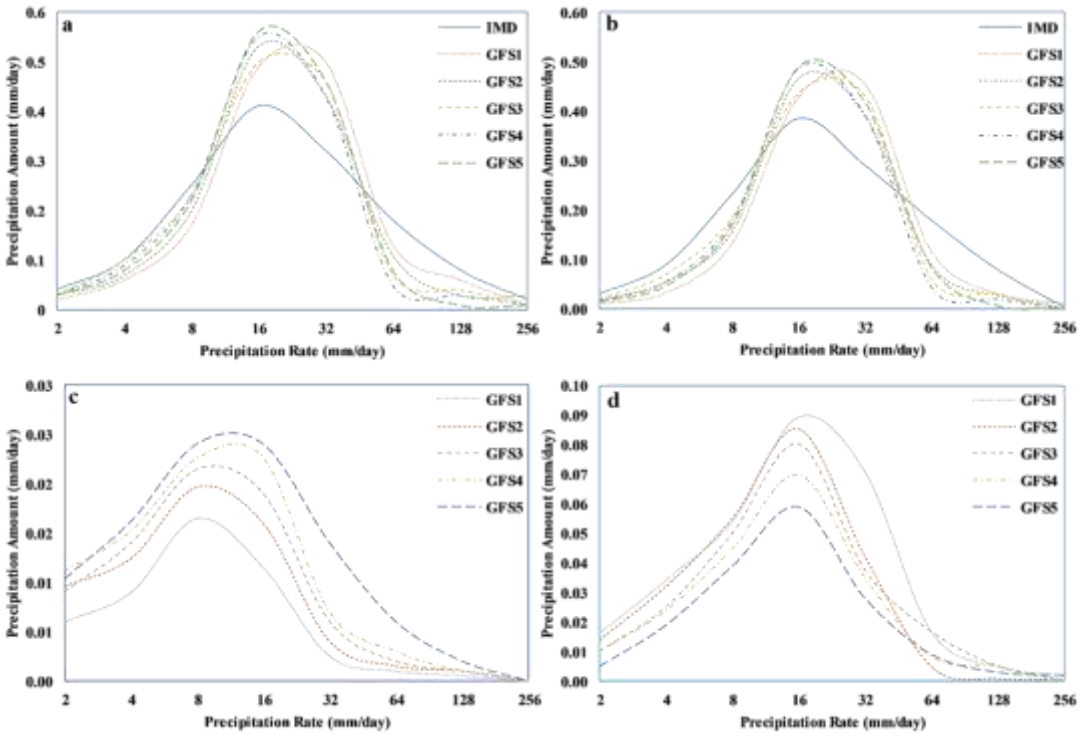

Fig. 10. Intensity distribution plots of GFS five-day (i.e., day-1 to day-5) rainfall forecast over the Nagavali and Vamsadhara basins: a) Total Rainfall, b) Hit Rainfall, c) Missed Rainfall, and d) False Rainfall.

e. Bias Correction of Rainfall

The GFS rainfall forecasts were corrected for bias using the simple multiplication scheme mentioned in section 4.4. Bias factors were calculated and verified by dividing the entire dataset into two parts: dataset-1 (from June 2015 to December 2018) and dataset-2 (from January 2019 to December 2020). The bias factors were calculated with dataset1 and validated with dataset2. The intensity distribution plots (Fig. 6(a) and 6(b)) show that the GFS model overestimated the rainfall events with intensities greater than 12mm/day, resulting in false alarms. The categorical rainfall thresholds chosen for calculating the bias factors are 8mm, 12mm, 16mm, and 20mm. The dataset-1 was divided into two groups for each threshold. For

instance, to calculate the bias factor at a threshold of 8mm, the dataset-1 was divided into two groups as rainfall less than or equal to 8 mm/day and greater than 8 mm/day. The bias factors for rainfall forecasts from day-1 to day-5 for both the Nagavali and Vamsadhara basins at different thresholds are presented in Table 2. To avoid underestimation of rainfall, the bias factors were applied to dataset-2 for rainfall events with intensity greater than the threshold value.

Forecast day	RI ≤ 8	RI > 8	RI ≤ 12	RI > 12	RI ≤ 16	RI > 16	RI ≤ 20	RI > 20
GFS1	1.059	0.612	0.888	0.648	0.727	0.655	1.059	0.612
GFS2	0.987	0.717	0.888	0.787	0.762	0.801	0.987	0.717
GFS3	0.936	0.831	0.891	0.891	0.779	1.004	0.936	0.831
GFS4	0.681	0.933	0.854	0.877	0.698	1.203	0.681	0.933
GFS5	0.940	0.765	0.853	0.833	0.754	0.899	0.940	0.765

Note: RI indicates rainfall intensity in mm/day

Table 2. Calculated bias factors for the GFS five-day (i.e., day-1 to day-5) rainfall forecasts using IMD gridded observed data from June 2015 to December 2018 over the Nagavali and Vamsadhara basins.

After recalculating the statistical indices for the bias corrected GFS rainfall forecasts, skill scores were calculated to see if there was an improvement in the forecast after the bias correction. The skill scores for the statistical indices at different threshold values are presented in Table 3.The magnitude of CC over both the Nagavali and Vamsadhara basins improved slightly at all threshold values after bias correction as per Table 2. Based on the skill score values of BIAS, RMSE, and ME in both basins, a significant improvement was observed after the bias correction at all threshold values. Over the Nagavali basin, the improvement in BIAS and ME ranged between 38 – 64%, 44 – 65%, 22 – 53%, and 3 – 53% at thresholds of 8, 12, 16, and 20 mm/day, respectively with a maximum improvement on day-1 forecast. The RMSE is improved by a maximum of 23%, 23%, 21% and 17% for the day-1 forecast at thresholds of 8, 12, 16, and 20 mm/day, respectively. From day-2 to day-5, the improvement in RMSE is ranged between 4 – 8%, 5 – 9%, 3 – 7%, and 0 – 5% at thresholds of 8, 12, 16, and 20 mm/day, respectively. Over the Vamsadhara basin, the improvement in BIAS and ME ranged between

14 – 57%, 65 – 93%, 31 – 68%, and 4 – 42% at thresholds of 8, 12, 16, and 20 mm/day, respectively. The improvement in RMSE is ranged between 2 – 18%, 3 – 18%, 2 – 16%, and 0 – 14% at the respective threshold values. From the skill score values, it was observed that the bias correction for rainfall with intensity greater than 12 mm/day in both basins has shown the highest improvement when compared with the other thresholds.

Forecast Day	Nagavali Basin			Vamsadhara Basin		
	BIAS	**RMSE**	**ME**	**BIAS**	**RMSE**	**ME**
	8/12/16/20	**8/12/16/20**	**8/12/16/20**	**8/12/16/20**	**8/12/16/20**	**8/12/16/20**
Day-1	64/65/57/53	23/23/21/17	64/65/57/53	57/7758/42	18/18/16/14	57/77/58/42
Day-2	59/62/38/22	8/9/7/5	59/62/38/22	24/93/58/34	5/5/4/3	24/93/58/34
Day-3	38/44/22/3	4/5/1/0	38/44/22/3	16/76/68/5	2/3/2/0	16/76/68/5
Day-4	43/49/23/3	5/5/3/0	43/49/23/3	14/65/31/4	3/3/2/0	14/65/31/4
Day-5	52/53/29/11	7/7/5/2	52/53/29/11	15/85/46/18	3/3/2/1	15/85/46/18

Note: 8/12/16/20 indicates the threshold values considered for the calculation of bias factors and 64/65/57/53 indicates the improvement in the model forecast after the bias correction at respective threshold values.

Table 3. Percentage improvement in the statistical indices of GFS five-day (i.e., day-1 to day-5) rainfall forecast for the study basins over a two-year period (i.e., from January 2019 to December 2020).

To further investigate the influence of bias correction of GFS rainfall forecasts over both basins, the spatial distribution of statistical indices before and after the bias correction are presented in Fig. 11 and 12. From the spatial patterns of spatial indices, it was evident that the magnitude of CC has improved from day-1 to day-5 in all parts of both basins after bias correction. For the day-1 and day-2 forecasts, the maximum improvement in CC was observed in the lower parts of both basins. Whereas, from day-3 to day-5 the improvement in CC was observed in all parts of both basins. From the spatial patterns of BIAS, it was observed that the overestimation of rainfall has decreased significantly from day-1 to day-5 in all parts of both basins. For day-1 forecasts, before the bias correction, the overestimation ranged from 55 % to 90% in the middle and upper portions of the Nagavali basin and in the middle portion of the Vamsadhara basin. After the bias correction, the overestimation in the middle and upper

portions of the Nagavali basin and in the middle portion of the Vamsadhara basin has decreased to 21 – 38%. Similarly, from day-2 to day-5 the overestimation of rainfall has decreased significantly in all parts of both basins. The spatial patterns of the ME followed the similar patterns of BIAS in both Nagavali and Vamsadhara basins. Spatial patterns of RMSE showed that its magnitude had decreased significantly from day-1 to day-5 in all parts of both basins after bias corrections. The spatial patterns of ME followed the similar of BIAS in both the basins.

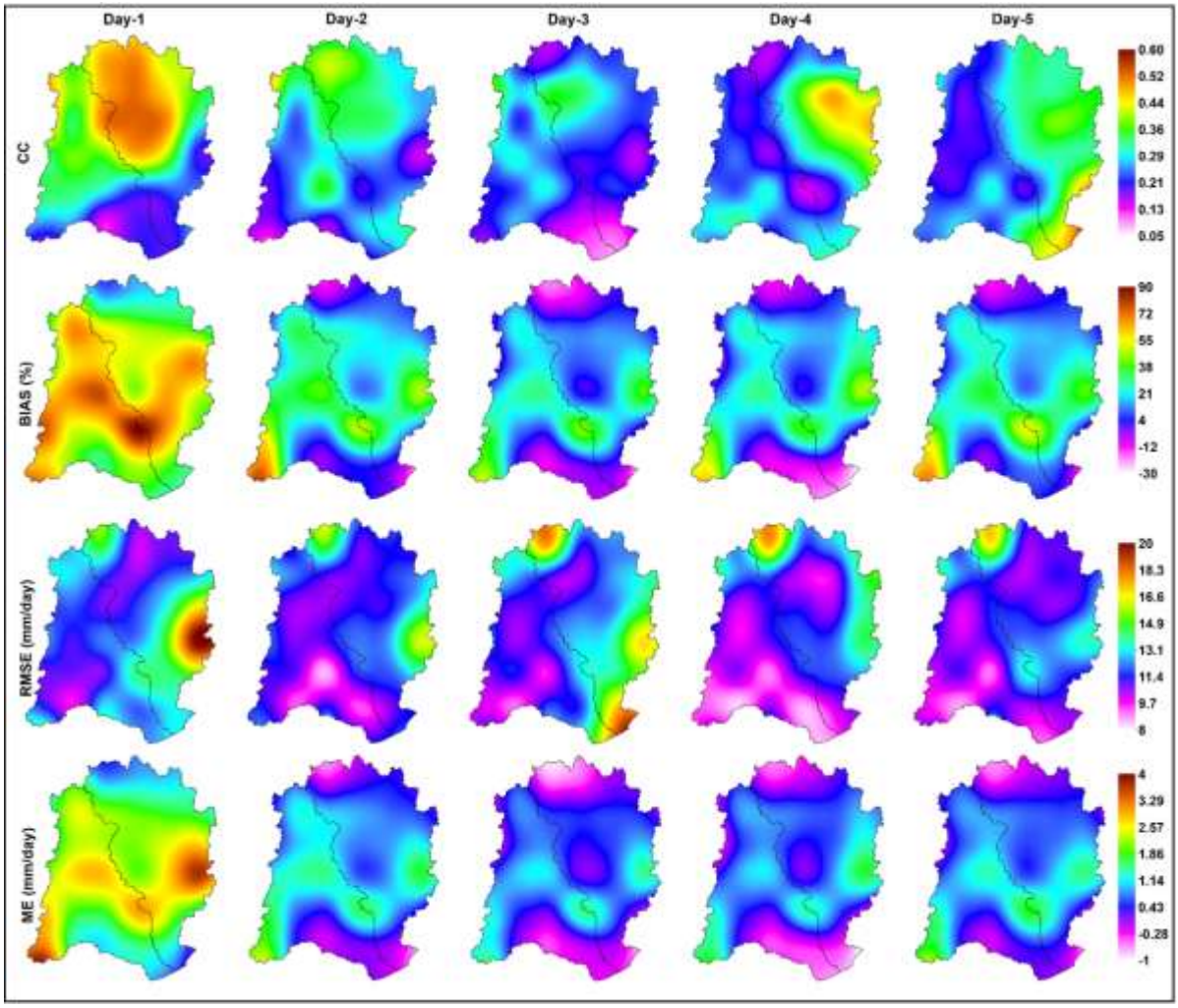

Fig. 11. Spatial plot of Correlation Coefficient (CC), Relative Bias (BIAS), Root Mean Square Error (RMSE), and Mean Error (ME) for the dataset-2 before the bias corrections

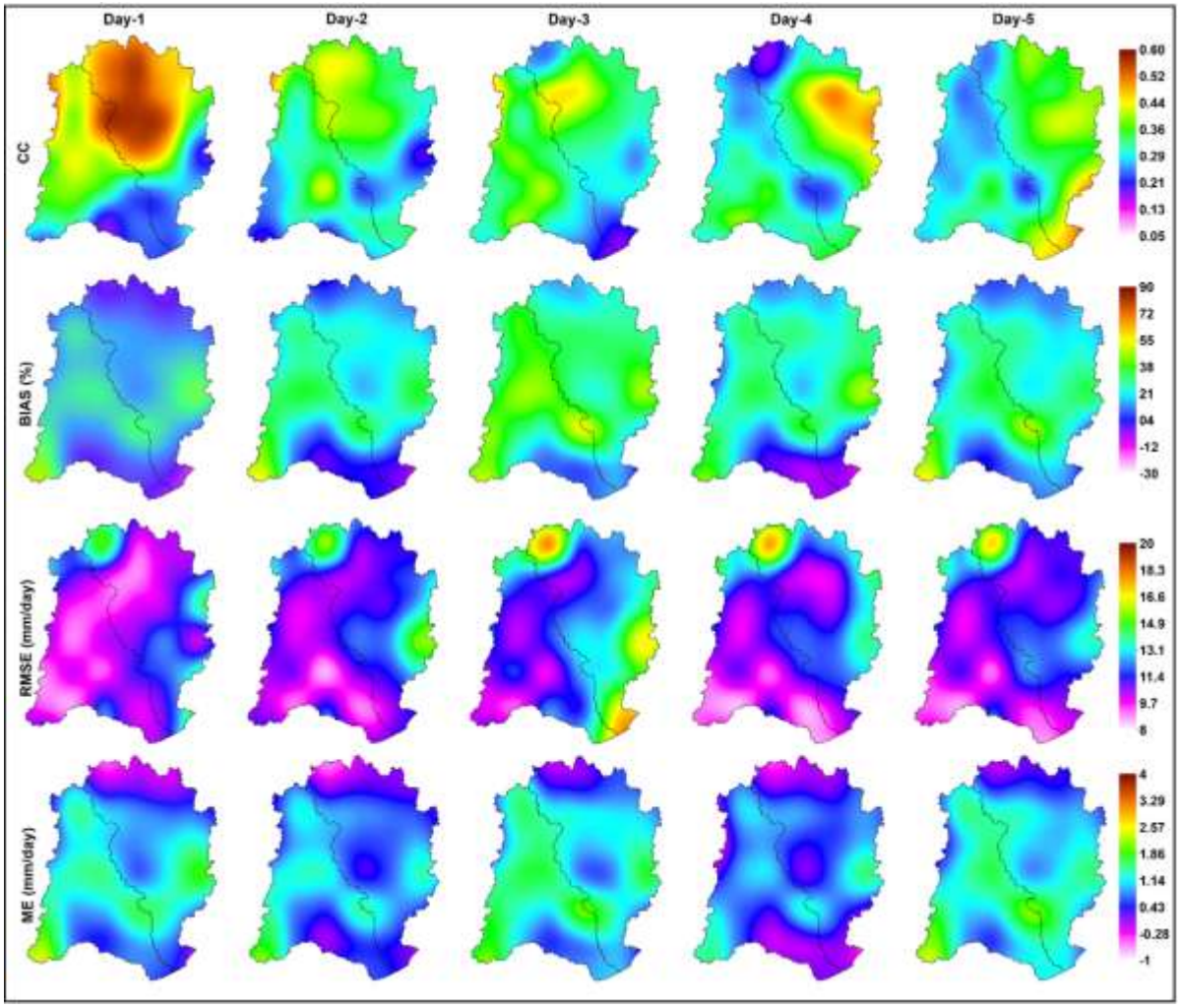

Fig 12. Spatial plot of Correlation Coefficient (CC), Relative Bias (BIAS), Root Mean Square Error (RMSE), and Mean Error (ME) for the dataset-2 after the bias correction

6. Conclusions

The Nagavali and Vamsadhara basins experienced frequent floods as a result of heavy rainfall during the southwest monsoon and tropical cyclones during the pre- and post-monsoon seasons. Precise and accurate rainfall forecasts will help the farmers in planning their day-to-day agricultural operations, and the government agencies in issuing early warnings during flood events. In view of this, in the present study, the skill of NCEP GFS model to forecast rainfall was examined using statistical metrics (correlation coefficient, relative bias, root-mean-square-error, and mean error), as well as contingency statistics (probability of detection, false alarm ratio, critical success index, and true skill score). The model performed well in forecasting rainfall over both the Nagavali and Vamsadhara basins. For day-1 to day-3, the model showed a correlation of greater than 0.3 with respect to the observed data, with probability of detection

greater than 0.6. The model overestimated the rainfall on day-1, and as the lead time increased, the overestimation became an underestimation. From the error decomposition, HB and FB significantly contributed to total error at the beginning of the forecast, and the contribution of MB has increased with lead time. A total of four threshold values (8mm, 12mm, 16mm, and 20mm) were chosen to calculate the bias factors and the maximum improvement in the GFS model forecasts was observed when the bias correction for rainfall events with intensity greater than 12 mm/day was applied. Finally, the present study recommends that the GFS rainfall forecasts be corrected for bias before being used as input to hydrological models. The outcome of the present study will be useful in understanding the characteristics of forecasted rainfall. The current study's findings will also help to improve the forecasting capabilities of hydrological models and will aid in effective management of available water resources in the basins. The methodology presented in the manuscript can be extended to other flood-prone basins.

Funding

The research described in this paper was carried out with fund made available by Ministry of Human Resource Development (MHRD), Government of India under the Scheme for Promotion of Academic and Research Collaboration (SPARC) through project number P270.

Acknowledgments.

The public access to the gridded rainfall data provided by India Meteorological Department and rainfall forecasts provided by National Center for Environmental Prediction (NCEP) Global Forecast System (GFS) are gratefully acknowledged. The corresponding author acknowledges the support by the Virginia Agricultural Experiment Station (Blacksburg) and the Hatch Program of the National Institute of Food and Agriculture, U.S. Department of Agriculture (Washington, D.C.).

Data Availability Statement.

Datasets used in the present study are available in a public repository.

All the observed data used during this study are openly available from IMD data center at https://www.imdpune.gov.in/Clim_Pred_LRF_New/Grided_Data_Download.html. The GFS rainfall forecasts used in the present study are openly available from NCAR Research Data Archive Computational & Information Systems Lab at https://rda.ucar.edu/datasets/ds084.1/.

REFERENCES

APSDMA, 2017. District disaster management plan of Srikakulam: General plan and hazard vulnerability and capacity analysis.

Ashrit, R., Sharma, K., Kumar, Sushant, Dube, A., Karunasagar, S., Arulalan, T., Mamgain, A., Chakraborty, P., Kumar, Sumit, Lodh, A., Dutta, D., Momin, I., Bushair, M.T., Prakash, B.J., Jayakumar, A., Rajagopal, E.N., 2020. Prediction of the August 2018 heavy rainfall events over Kerala with high-resolution NWP models . Meteorol. Appl. 27, 1–14. https://doi.org/10.1002/met.1906

Bhowmik, S.K.R., Joardar, D., Hatwar, H.R., 2007. Evaluation of precipitation prediction skill of IMD operational NWP system over Indian monsoon region. Meteorol. Atmos. Phys. 95, 205–221. https://doi.org/10.1007/s00703-006-0198-3

Broorks, H., Brown, B., Ebert, B., Ferro, C., Jolliffe, I., Koh, T.-Y., Roebber, P., Stephenson, D., 2017. Forecast Verification methods Across Time and Space Scales [WWW Document]. URL https://www.cawcr.gov.au/projects/verification/

Cho, D., Yoo, C., Im, J., Cha, D.H., 2020. Comparative Assessment of Various Machine Learning-Based Bias Correction Methods for Numerical Weather Prediction Model Forecasts of Extreme Air Temperatures in Urban Areas. Earth Sp. Sci. 7. https://doi.org/10.1029/2019EA000740

Damrath, U., Doms, G., Frühwald, D., Heise, E., Richter, B., Steppeler, J., 2000. Operational quantitative precipitation forecasting at the German Weather Service. J. Hydrol. 239, 260–285. https://doi.org/10.1016/S0022-1694(00)00353-X

DC, 2017. Nagavali, Vamsadhara inflows recede; flash floods threat looms. Deccan Chron.

Deng, P., Zhang, M., Guo, H., Xu, C., Bing, J., Jia, J., 2018. Error analysis and correction of the daily GSMaP products over Hanjiang River Basin of China. Atmos. Res. 214, 121–134. https://doi.org/10.1016/j.atmosres.2018.07.022

Dube, A., Ashrit, R., Ashish, A., Sharma, K., Iyengar, G.R., Rajagopal, E.N., Basu, S., 2014. Forecasting the heavy rainfall during Himalayan flooding-June 2013. Weather Clim. Extrem. 4, 22–34. https://doi.org/10.1016/j.wace.2014.03.004

Durai, V.R., Bhardwaj, R., Roy Bhowmik, S.K., Rama Rao, Y. V., 2015. Verification of quantitative precipitation forecasts from operational ensemble prediction systems over India. Mausam 66, 479–496.

572 Durai, V.R., Bhowmik, S.K.R., 2014. Prediction of Indian summer monsoon in short to
573 medium range time scale with high resolution global forecast system (GFS) T574 and
574 T382. Clim. Dyn. 42, 1527–1551. https://doi.org/10.1007/s00382-013-1895-5

575 Durai, V.R., Bhradwaj, R., 2014. Evaluation of statistical bias correction methods for
576 numerical weather prediction model forecasts of maximum and minimum temperatures.
577 Nat. Hazards 73, 1229–1254. https://doi.org/10.1007/s11069-014-1136-1

578 Durai, V.R., Das, A.K., 2019. NWP products for monsoon weather monitoring and prediction
579 at various temporal / spatial scales, in: Monsoon: A Report 2019. pp. 134–162.

580 Durai, V.R., Roy Bhowmik, S.K., Mukhopadhyay, B., 2010. Performance evaluation of
581 precipitation prediction skill of NCEP global Forecasting System (GFS) over Indian
582 region during summer monsoon 2008. Mausam 61, 139–154.

583 Ebert, E.E., 2001. Ability of a poor man's ensemble to predict the probability and distribution
584 of precipitation. Mon. Weather Rev. 129, 2461–2480. https://doi.org/10.1175/1520-
585 0493(2001)129<2461:AOAPMS>2.0.CO;2

586 Fan, Y., van den Dool, H., 2011. Bias Correction and Forecast Skill of NCEP GFS Ensemble
587 Week-1 and Week-2 Precipitation, 2-m Surface Air Temperature, and Soil Moisture
588 Forecasts. Weather Forecast. 26, 355–370. https://doi.org/10.1175/WAF-D-10-05028.1

589 Ganai, M., Tirkey, S., Krishna, R.P.M., Mukhopadhyay, P., 2021. The impact of modified rate
590 of precipitation conversion parameter in the convective parameterization scheme of
591 operational weather forecast model (GFS T1534) over Indian summer monsoon region.
592 Atmos. Res. 248, 105185. https://doi.org/10.1016/j.atmosres.2020.105185

593 Guo, R., Yu, H., Yu, Z., Tang, J., Bai, L., 2021. Application of the frequency-matching method
594 in the probability forecast of landfalling typhoon rainfall. Front. Earth Sci.
595 https://doi.org/10.1007/s11707-021-0880-2

596 Lekula, M., Lubczynski, M.W., Shemang, E.M., Verhoef, W., 2018. Validation of satellite-
597 based rainfall in Kalahari. Phys. Chem. Earth 105, 84–97.
598 https://doi.org/10.1016/j.pce.2018.02.010

599 Mandal, V., De, U.K., Basu, B.K., 2007. Precipitation forecast verification of the Indian
600 Summer Monsoon with Intercomparison of Three Diverse Regions. Weather Forecast. 22,
601 428–443. https://doi.org/10.1175/WAF1010.1

602 Mccorkle, T.A., Horel, J.D., Jacques, A.A., Alcott, T., 2018. Evaluating the experimental High-

603 Resolution Rapid Refresh-Alaska modeling system using US array pressure observations.
604 Weather Forecast. 33, 933–953. https://doi.org/10.1175/WAF-D-17-0155.1

605 Mukhopadhyay, P., Prasad, V.S., Krishna, R.P.M., Deshpande, M., Ganai, M., Tirkey, S.,
606 Sarkar, S., Goswami, T., Johny, C.J., Roy, K., Mahakur, M., Durai, V.R., Rajeevan, M.,
607 2019. Performance of a very high-resolution global forecast system model (GFS T1534)
608 at 12.5 km over the Indian region during the 2016–2017 monsoon seasons. J. Earth Syst.
609 Sci. 128, 1–18. https://doi.org/10.1007/s12040-019-1186-6

610 Ning, S., Song, F., Udmale, P., Jin, J., Thapa, B.R., Ishidaira, H., 2017. Error Analysis and
611 Evaluation of the Latest GSMap and IMERG Precipitation Products over Eastern China.
612 Adv. Meteorol. 2017. https://doi.org/10.1155/2017/1803492

613 Pai, D.S., Sridhar, L., Rajeevan, M., Sreejith, O.P., Satbhai, N.S., Mukhopadhyay, B., 2014.
614 Development of a new high spatial resolution (0.25° × 0.25°) long period (1901-2010)
615 daily gridded rainfall data set over India and its comparison with existing data sets over
616 the region. Mausam 65, 1–18.

617 Prakash, S., Mitra, A.K., AghaKouchak, A., Liu, Z., Norouzi, H., Pai, D.S., 2018. A
618 preliminary assessment of GPM-based multi-satellite precipitation estimates over a
619 monsoon dominated region. J. Hydrol. 556, 865–876.
620 https://doi.org/10.1016/j.jhydrol.2016.01.029

621 Prakash, S., Mitra, A.K., Momin, I.M., Rajagopal, E.N., Milton, S.F., Martin, G.M., 2016a.
622 Skill of short- to medium-range monsoon rainfall forecasts from two global models over
623 India for hydro-meteorological applications. Meteorol. Appl. 23, 574–586.
624 https://doi.org/10.1002/met.1579

625 Prakash, S., Momin, I.M., Mitra, A.K., Bhattacharjee, P.S., Yang, F., Tallapragada, V., 2016b.
626 An Early Assessment of Medium Range Monsoon Precipitation Forecasts from the Latest
627 High-Resolution NCEP-GFS (T1534) Model over South Asia. Pure Appl. Geophys. 173,
628 2215–2225. https://doi.org/10.1007/s00024-016-1248-5

629 Rao, G.V., Reddy, K.V., Sridhar, V., 2020a. Sensitivity of microphysical schemes on the
630 simulation of post-monsoon tropical cyclones over the north Indian Ocean. Atmosphere
631 (Basel). 11, 1–17. https://doi.org/10.3390/atmos11121297

632 Rao, G.V., Venkata Reddy, K., Srinivasan, R., Sridhar, V., Umamahesh, N. V., Pratap, D.,
633 2020b. Spatio-temporal analysis of rainfall extremes in the flood-prone Nagavali and

Vamsadhara Basins in eastern India. Weather Clim. Extrem. 29, 100265. https://doi.org/10.1016/j.wace.2020.100265

Satyanarayana, G.C., Kar, S.C., 2016. Medium-range forecasts of extreme rainfall events during the Indian summer monsoon. Meteorol. Appl. 23, 282–293. https://doi.org/10.1002/met.1553

Saulo, A.C., Seluchi, M., Campetella, C., Ferreira, L., 2001. Error evaluation of NCEP and LAHM regional model daily forecasts over southern South America. Weather Forecast. 16, 697–712. https://doi.org/10.1175/1520-0434(2001)016<0697:EEONAL>2.0.CO;2

Setti, S., Maheswaran, R., Radha, D., Sridhar, V., Barik, K.K., Narasimham, M.L., 2020. Attribution of Hydrologic Changes in a Tropical River Basin to Rainfall Variability and Land-Use Change: Case Study from India. J. Hydrol. Eng. 25, 05020015. https://doi.org/10.1061/(asce)he.1943-5584.0001937

Shahrban, M., Walker, J.P., Wang, Q.J., Seed, A., Steinle, P., 2016. An evaluation of numerical weather prediction based rainfall forecasts. Hydrol. Sci. J. 61, 2704–2717. https://doi.org/10.1080/02626667.2016.1170131

Sharma, K., Ashrit, R., Bhatla, R., Mitra, A.K., Iyengar, G.R., Rajagopal, E.N., 2017. Skill of Predicting Heavy Rainfall Over India: Improvement in Recent Years Using UKMO Global Model. Pure Appl. Geophys. 174, 4241–4250. https://doi.org/10.1007/s00024-017-1640-9

Sharma, K., Ashrit, R., Ebert, E., Iyengar, G., Mitra, A., 2015. NGFS rainfall forecast verification over India using the contiguous rain area (CRA) method. Mausam 66, 415–422.

Sharma, K., Ashrit, R., Kumar, S., Milton, S., Rajagopal, E.N., Mitra, A.K., 2021. Unified model rainfall forecasts over India during 2007–2018: Evaluating extreme rains over hilly regions. J. Earth Syst. Sci. 130. https://doi.org/10.1007/s12040-021-01595-1

Singh, D., Bhutiyani, M.R., Ram, T., 2014. Station-based verification of qualitative and quantitative mm5 precipitation forecasts over northwest himalaya (Nwh). Meteorol. Atmos. Phys. 125, 107–118. https://doi.org/10.1007/s00703-014-0321-9

Sridevi, C., Singh, K.K., Suneetha, P., Durai, V.R., Kumar, A., 2020. Rainfall forecasting skill of GFS model at T1534 and T574 resolution over India during the monsoon season. Meteorol. Atmos. Phys. 132, 35–52. https://doi.org/10.1007/s00703-019-00672-x

Sridevi, C., Singh, K.K., Suneetha, P., Durai, V.R., Kumar, A., 2018. Rainfall forecast skill of Global Forecasting System (GFS) model over India during summer monsoon 2015. Geofizika 35, 39–52. https://doi.org/10.15233/gfz.2018.35.4

Sun, Q., Miao, C., Duan, Q., Ashouri, H., Sorooshian, S., Hsu, K.L., 2018. A Review of Global Precipitation Data Sets: Data Sources, Estimation, and Intercomparisons. Rev. Geophys. 56, 79–107. https://doi.org/10.1002/2017RG000574

Tian, Y., Peters-Lidard, C.D., Eylander, J.B., Joyce, R.J., Huffman, G.J., Adler, R.F., Hsu, K.L., Turk, F.J., Garcia, M., Zeng, J., 2009. Component analysis of errors in Satellite-based precipitation estimates. J. Geophys. Res. Atmos. 114, 1–15. https://doi.org/10.1029/2009JD011949

Wang, S., Yu, L., Zhu, S., 2020. Precipitation forecast on the township scale using the frequency matching method. IOP Conf. Ser. Earth Environ. Sci. 467. https://doi.org/10.1088/1755-1315/467/1/012050

World Meteorological Organization, 1977. Manual on the Global Data-Processing System: Global Aspects, WMO ; no. 485.

Yang, C., Yuan, H., Su, X., 2020. Bias correction of ensemble precipitation forecasts in the improvement of summer streamflow prediction skill. J. Hydrol. 588, 124955. https://doi.org/10.1016/j.jhydrol.2020.124955

Zarei, M., Najarchi, M., Mastouri, R., 2021. Bias correction of global ensemble precipitation forecasts by Random Forest method. Earth Sci. Informatics 14, 677–689. https://doi.org/10.1007/s12145-021-00577-7

Zhu., Y., Toth, Z., 2004. Implementation of bias-corrected QPF and PQPF forecasts. NOAA/NWS/Environmental Modeling Center [WWW Document]. URL http://wwwt.emc.ncep.noaa.gov/gmb/ens/index.html

Zhu, Y., Luo, Y., 2015. Precipitation calibration based on the frequency-matching method. Weather Forecast. 30, 1109–1124. https://doi.org/10.1175/WAF-D-13-00049.1